Rare Metal Materials and Engineering
Volume 50, Issue 3, March 2021
Available online at www.rmme.ac.cn

Science Press

Cite this article as: Rare Metal Materials and Engineering, 2021, 50(3): 0860-0866.

ARTICLE

Effect of Nb on Microstructure and Mechanical Properties of Fe-28Mn-10Al-C Low-Density Steel

Ma Tao[1], Gao Jianxin[1], Li Huirong[1], Meng Xianghai[1,2], Li Yungang[1]

[1] College of Metallurgy and Energy, North China University of Science and Technology, Tangshan 063210, China; [2] Tangshan Polytechnic College, Tangshan 063210, China

Abstract: A novel Fe-28Mn-10Al-C-0.5Nb low-density steel containing 0.5wt% Nb for automobile was developed, aiming to study the effect of Nb addition on the structure and mechanical properties of austenitic Fe-Mn-Al-C low-density steel. With the addition of Nb, the average austenite grain size in Fe-28Mn-10Al-C low-density steel is refined from 39.49 μm to 13.67 μm, and the formation of twins is also suppressed. Besides, the yield strength and ultimate tensile strength of Fe-28Mn-10Al-C low-density steel increase by 171 and 64 MPa, respectively, and the elongation after fracture increases by 11.5%, revealing an excellent balance of strength and ductility. This is due to the precipitation strengthening of NbC precipitates and fine grain strengthening of austenite. Precipitation strengthening plays an important role to increase the yield strength of Nb-added low-density steel.

Key words: Fe-Mn-Al-C; Nb; NbC; grain refinement; tensile property

With the development of the automobile industry, fuel consumption and emission pollution problems have aroused concern. As a solution, reducing the mass of cars by safe and lightweight steel can decrease the fuel consumption and pollution effectively. Fe-Mn-Al-C steel prepared by adding Al to Mn-rich austenitic steel can be used in automobile manufacturing to realize the mass loss of automobile[1,2] due to its low-density, excellent mechanical properties, formability and weldability. Therefore, it is widely concerned around the world[3-5].

Compared with transformation induced plasticity (TRIP) steel and twin-induced plasticity (TWIP) steel, the Al content in Fe-Mn-Al-C steel is usually more than 10wt%, which is beneficial to achieve mass loss and better mechanical properties. This is because the addition of Al increases the stacking fault energy (SFE)[6] of Mn-rich austenitic steel, making plane slip become the main deformation mechanism. In addition, the addition of Al also induces dynamic precipitation of κ-carbide. $L1_2$ type κ-carbides with face-centered cubic structure precipitated through spinodal decomposition of austenite. Through precipitation strengthening of κ-carbides, dislocation plane slip is prevented, and the mechanical properties of low-density steel improve. Sutou et al[7] reported that the fine κ-carbides produced during the quenching process improve the yield strength and tensile strength while maintaining high ductility of Fe-20Mn-(10, 11)Al-(1.0,1.5)C low-density steel. Kalashnikov[8] reported that when the Al content exceeds 7wt%, the austenitic Fe-Mn-Al-C steel after aging treatment is significantly strengthened due to the precipitation of nano-scale κ-carbides with elevated yield strength and ultimate tensile strength. However, the strengthening effect of κ-carbides on low-density steel is affected by the shape and distribution position. Research shows that due to the stress concentration at the grain boundary, coarse κ-carbides distributed along grain boundaries reduce the ductility of low-density steel[9,10]. Sutou et al[7] found that when fine nano-scale particles of κ-carbides were uniformly distributed in Fe-20Mn-11Al-1.2C steel, low-density steel exhibits strong strain hardening with high yield strength (530 MPa) and high elongation (59.1%). As the κ-carbide coars-

Received date: October 10, 2020
Foundation item: National Natural Science Foundation of China (51974129)
Corresponding author: Li Yungang, Ph. D., Professor, College of Metallurgy and Energy, North China University of Science and Technology, Tangshan 063210, P. R. China, Tel: 0086-315-8805420, E-mail: lyg@ncst.eud.cn

ens and the volume fraction increases, the strength of the material increases while the elongation decreases significantly (42%). Lu et al[11] reported that after aging treatment of Fe-Mn-Al-C steel at 600 ºC, fine dispersed κ-carbides greatly increase the hardness of steel. The coarse κ-carbides precipitated after high-temperature aging greatly reduce the ductility of low-density steel. Liu[12] confirmed that the fine and uniformly distributed κ-carbides precipitated by spinodal decomposition of austenite increase the work hardening rate of low-density Fe-11Mn-10Al-1.25C steel, which obtains a good balance between ductility and strength. Therefore, the size and distribution of κ-carbides need to be controlled to improve the mechanical properties of low-density steel, which limits its development and preparation for automobiles, and greatly increases the difficulty and cost of production.

Nb has many applications in steel[13,14]. As a strong carbide forming element, Nb can form stable NbC phases and refine the austenite grain size, which makes it widely used in steel. By micro-alloying with Nb in austenitic Fe-Mn-Al-C low-density steel, NbC precipitates uniformly distributed in austenite can be obtained, and the size of austenite grain can be refined. The mechanical properties of low-density steel can be optimized by precipitation strengthening and fine grain strengthening through the NbC precipitation. In addition, due to the strong stability of NbC, it can maintain the nano-scale particle size during the high-temperature aging process, and effectively avoid the reduction of ductility caused by the coarsening of the precipitated phase. Moreover, because Nb has a strong affinity for C, NbC phase forms by consuming C atoms in the steel, which inhibits the spinodal decomposition of austenite. The precipitation and growth of κ-carbides can also be restrained to avoid coarsening and damage to the mechanical properties of low-density steel. Besides, the addition of a trace amount of Nb cannot cause a significant increase of density of Fe-Mn-Al-C steel. Therefore, the present work aims to develop a novel low-density Fe-Mn-Al-C-Nb steel. The effect of Nb addition on the microstructure and properties of low-density steel were studied. These results provided theoretical support for Nb alloyed low-density steel.

1 Experiment

The composition of the low-density steel used in this work is shown in Table 1. Except for the Nb content, the composition of the two steels is basically the same, which are marked as A and B, respectively. A 25 kg ingot was prepared by induction melting in the argon atmosphere. The ingot was heated at 1150 °C for 2 h, and then forged into a slab with sectional dimension of 80 mm×40 mm. After homogenization at 1200 °C for 2 h, the slab was hot rolled to a plate with thickness of 5 mm. Then the hot rolled plate was solution treated at 950 °C for 1 h and water quenched to room temperature. According to the Archimedes principle, the density of steel A and B was measured by densitometry (Byes-300A), and is 6.30 and 6.63 g/cm^3, respectively, which is 19% and 15% lower than the density of pure iron.

Specimens for tensile test with the dimension of 25 mm×5 mm×6 mm were machined from the hot-rolled plate along the direction parallel to the rolling direction. The tensile test was carried out at room temperature on the universal testing machine (INSTRON 3382) at an initial strain rate of 1×10^{-3} s^{-1}.

The microstructure observation and analysis of the characteristics of the precipitated phase were performed by the optical microscope (OM, Leica DMi8), scanning electron microscope (SEM, Quanta 650), and transmission electron microscope (TEM, Tecnai G2 F20 S-TWIN). The specimens used for OM and SEM observation were mechanically polished and then etched with 4vol% nital. Thin foils for TEM analysis were electro-polished by a twin-jet polishing using a mixture of 10vol% perchloric acid and 90vol% ethanol with an applied voltage of 20 V at −35 °C. TEM observation was performed at 200 kV.

2 Results and Discussion

2.1 Microstructure

The optical micrographs of the samples after solution treatment are shown in Fig.1. Both A (Fig.1a) and B (Fig.1b) steels show the stable austenite structure, and the twins form. It can be seen that the austenite grain size of steel A without Nb is obviously large. The average grain size of steel A and steel B is 39.49 and 13.67 μm, respectively. In addition, compared with steel A without Nb, steel B with 0.5wt% Nb has fewer twins.

Fig.2 shows the SEM morphologies and EDS analysis of B steel. As can be seen from Fig.2a, by adding a small amount of Nb to the low-density steel, precipitated phases form, and are distributed continuously along the austenite grain boundaries. The EDS element mapping results show that the distribution positions of Nb and C are almost the same, indicating that the precipitates are NbC. In order to further analyze the morphologies of the precipitated phases, Fig.3 shows the bright-field TEM images and selected-area electron diffraction patterns (SAEDPs) of B steel. Analysis of SADPs indicates that, after solution treated at 950 °C, satellite spot distribution near the main diffraction spot, indicates that the action of spinodal decomposition of austenite takes place, and the ordered phase with the same structure as austenite formed. In addition, lattice constant also change accordingly. Besides, as is shown by bright-field TEM images, the second phase will precipitate in B steel after solution treatment, which has ellipsoid shape. The precipitates are distributed in austenite grains and at grain boundaries, with a particle size of 450 nm and an ellipsoidal shape, and the EDS results show that the precipitates are NbC.

Table 1 Chemical composition of low-density steel (wt%)

Steel	C	Mn	Al	Nb	S	P	Fe
A	0.98	28.53	10.21	-	≤0.003	≤0.003	Bal.
B	1.05	29.82	10.95	0.56	≤0.003	≤0.003	Bal.

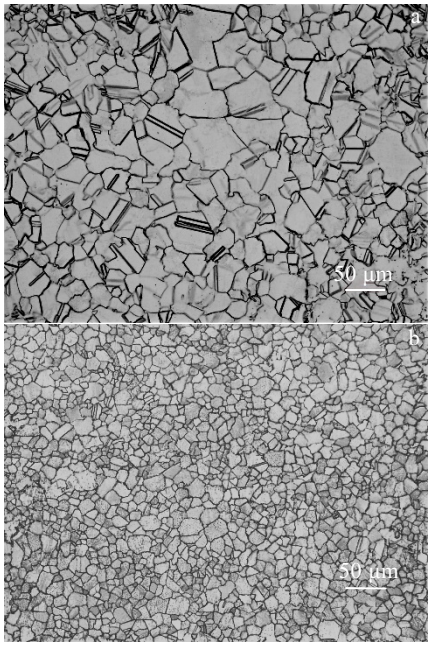

Fig.1 OM images of Fe-28Mn-10Al-C (a) and Fe-28Mn-10Al-C-0.5Nb (b) steel

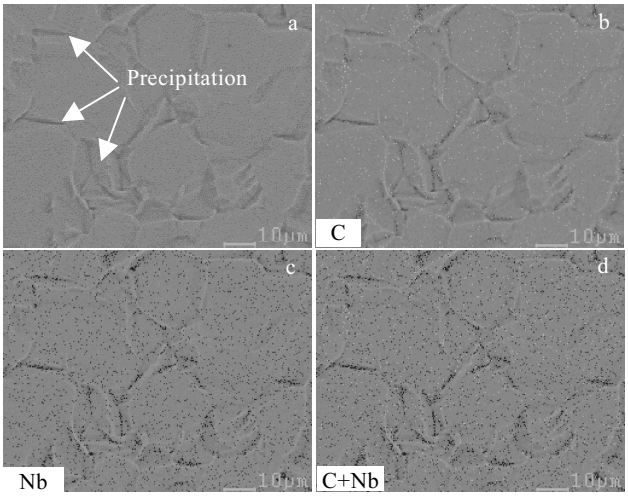

Fig.2 SEM image (a) and EDS element mapping (b~d) of Fe-28Mn-10Al-C-0.5Nb: (b) C; (c) Nb; (d) C and Nb

2.2 Stacking fault energy

It is known that Al can improve the stacking fault energy of Mn-rich austenitic steel. SFE determines the deformation mechanism of low-density steel, which further affects the mechanical properties. Based on the thermodynamic model established by Olson-Cohen, SFE (τ) can be estimated as follows:

$$\tau = 2\rho_{\Delta} G + 2\sigma \quad (1)$$

$$\rho = \left(\frac{4}{\sqrt{3}}\right)\left(\frac{1}{\alpha^2}\right) \quad (2)$$

where $\Delta G^{\gamma\to\varepsilon}$ is the Gibbs free energy for phase transition of γ_{fcc}, ρ is the molar planar density of {111} plane, σ is the γ/ε interfacial energy, α is the lattice constant of γ_{fcc}, and N is Avogadro number. For the single-phase (φ) binary solution composed of elements i and j, the Gibbs free energy G^{φ} can be expressed as follows:

$$G^{\varphi} = X_i G_i^{\varphi} + X_j G_j^{\varphi} + RT\left(X_i \ln X_i + X_j \ln X_j\right) + X_i X_j \Omega_{ij}^{\varphi} \quad (3)$$

$$\Omega_{ij}^{\varphi} = L_0^{\varphi} + L_1^{\varphi}\left(X_i - X_j\right) \quad (4)$$

$$G_{mg}^{\varphi} = f\left(\frac{T}{T_{neel}}\right) RT \ln\left(\beta + 1\right) \quad (5)$$

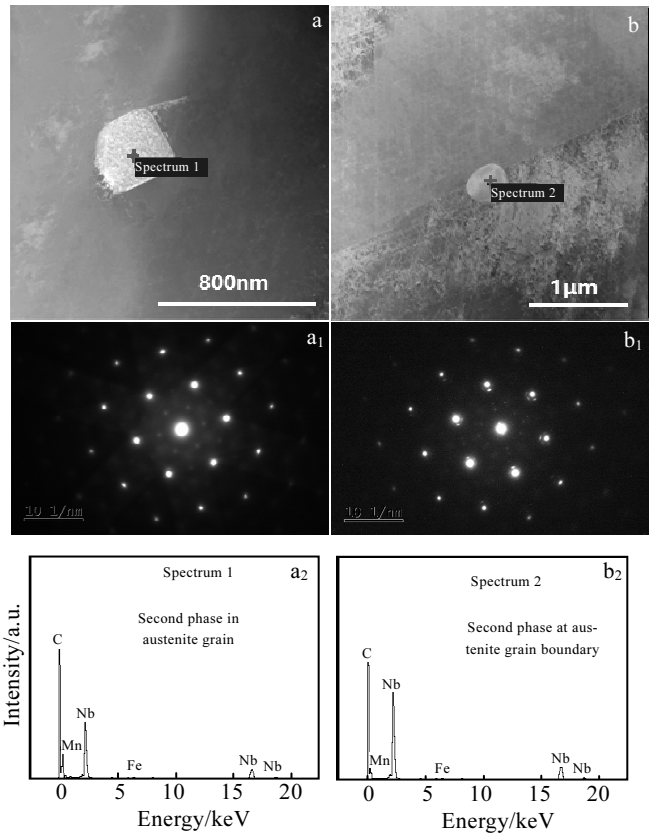

Fig.3 TEM bright field images (a, b), SAED patterns (a_1, b_1), and EDS analysis (a_2, b_2) second phase in grain of Fig.3a and at grain boundary of Fig.3b for Fe-28Mn-10Al-C-0.5Nb steel

where X is the mole fraction, G_{mg}^{φ} is the Gibbs free energy of φ phase in the magnetic state, L_0 is the temperature-based parameter, L_1 is the constant, T_{neel} is the Neel temperature, and β is the magnetic moment. By Eq.(3)~Eq.(5), the $\Delta G^{\gamma\to\varepsilon}$ for γ/ε transformation of the binary austenitic steel is given as follows:

$$\Delta G^{\gamma\to\varepsilon} = X_i\Delta G_i^{\gamma\to\varepsilon} + X_j\Delta G_j^{\gamma\to\varepsilon} + X_iX_j\Omega_{ij}^{\gamma\to\varepsilon} + \Delta G_{mg}^{\gamma\to\varepsilon} \quad (6)$$

According to Eq.(6) and the regular solid solution model, the Gibbs free energy of Fe-Mn-Al-C and Fe-Mn-Al-C-Nb low-density steel can be expressed as follows:

$$\begin{aligned}\Delta G^{\gamma\to\varepsilon} = {} & X_{Fe}\Delta G_{Fe}^{\gamma\to\varepsilon} + X_{Mn}\Delta G_{Mn}^{\gamma\to\varepsilon} + X_{Al}\Delta G_{Al}^{\gamma\to\varepsilon} \\ & + X_C\Delta G_C^{\gamma\to\varepsilon} + X_{Nb}\Delta G_{Nb}^{\gamma\to\varepsilon} + X_{Fe}X_{Mn}\Omega_{FeMn}^{\gamma\to\varepsilon} + \\ & X_{Fe}X_{Al}\Omega_{FeAl}^{\gamma\to\varepsilon} + X_{Fe}X_C\Omega_{FeC}^{\gamma\to\varepsilon} + X_{Fe}X_{Nb}\Omega_{FeNb}^{\gamma\to\varepsilon} + \\ & X_{Mn}X_C\Omega_{MnC}^{\gamma\to\varepsilon} + \Delta G_{mg}^{\gamma\to\varepsilon}\end{aligned} \quad (7)$$

Based on Eq.(1), Eq.(7), and the parameters and functions listed in Table 2[15], the $\Delta G^{\gamma\to\varepsilon}$ and SFE of A steel at room temperature are estimated as 1083 and 82 mJ/m^2, respectively. And for B steel with 0.5wt% Nb, the $\Delta G^{\gamma\to\varepsilon}$ and SFE are 1128 and 84 mJ/m^2, respectively.

2.3 Mechanical properties

Fig.4a shows the engineering stress-strain curves of steel A and B after solution treatment at 950 °C, and the corresponding properties are summarized in Table 3. Both steels exhibit continuous strain hardening effect, and high yield strength (YS) and ultimate tensile strengths (UTS). It is noteworthy that the UTS of both steel A and B is more than 1 GPa. With high strength, the elongation (EI) of steel A and B is 26.0% and 37.5%, respectively. Especially, with the addition of Nb, the YS and UTS of Fe-Mn-Al-C low-density steel increase by 171 and 64 MPa, respectively, and EI increases by 11.5%.

The product of strength and elongation (PSE=TS×ef) is usually used to describe the balance between ductility and strength. Among the low-density steels for automobile industries, the typical values of PSE for TRIP and TWIP steels are 15 and 20 GPa·%, respectively. It can be seen from Table 3 that after adding Nb to the Fe-Mn-Al-C low-density steel, the PSE increases from 26.52 to 40.65 GPa·%, which is much higher than that of the traditional TRIP and TWIP steels, indicating a good balance of strength and toughness.

The strain hardening rate (dσ/dε)-true stress (σ) curves of the A and B steels are presented in Fig.4b. When the true stress is less than 0.2 MPa, the steel A without Nb shows higher strain hardening rate. As the true strain continues to increase, the B steel with Nb maintains a continuously high dσ/dε value, which delays the plastic instability and thus has a better ductility.

3 Discussion

3.1 Existing form of Nb in Fe-Mn-Al-C-Nb steel

Based on the solid solubility theory of the second phase in steel materials, the solid solubility of Nb in steel is affected by C content and temperature of heat treatment. Moreover, the solid solubility of Nb in steel is extremely low, and most of Nb is precipitated as the second phase. Narita's[16] research confirmed that the stable compounds of Nb and non-metallic elements C and N form in steel. Meanwhile, these compounds have high solubility in steel.

Table 2 Relevant parameters for SFE estimation of Fe-28Mn-10Al-C and Fe-28Mn-10Al-C-0.5Nb steel[15]

Parameter	Value or related function
ρ/J·mol^{-1}	2.94×10^{-5}
σ/J·mol^{-1}	9
$\Delta G_{Fe}^{\gamma\to\varepsilon}$/J·mol^{-1}	$-2\,243.38+4.309T$
$\Delta G_{Mn}^{\gamma\to\varepsilon}$/J·mol^{-1}	$-1\,000+1.123T$
$\Delta G_{Al}^{\gamma\to\varepsilon}$/J·mol^{-1}	$2\,800+5T$
$\Delta G_{C}^{\gamma\to\varepsilon}$/J·mol^{-1}	−22 166
$\Delta G_{Nb}^{\gamma\to\varepsilon}$/J·mol^{-1}	4 046
$\Omega_{FeMn}^{\gamma\to\varepsilon}$/J·mol^{-1}	$2180+532(X_{Fe}-X_{Mn})$
$\Omega_{FeAl}^{\gamma\to\varepsilon}$/J·mol^{-1}	3 339
$\Omega_{FeC}^{\gamma\to\varepsilon}$/J·mol^{-1}	42 500
$\Omega_{MnC}^{\gamma\to\varepsilon}$/J·mol^{-1}	26 910
$\Omega_{FeNb}^{\gamma\to\varepsilon}$/J·mol^{-1}	27 403
β^{γ}	$0.7X_{Fe}+0.62X_{Mn}-0.64X_{Fe}X_{Mn}-4X_C$
β^{ε}	$0.62X_{Mn}-4X_C$
T_{nell}^{γ}	$580X_{Mn}$(K)
T_{nell}^{ε}	$250\ln X_{Mn}-4750X_{Mn}X_C-6.2X_{Al}+720$(K)
$f\left(\frac{T}{T_{nell}}\right)$	$1-\frac{\left[\left(\frac{79\tau^{-1}}{10}\right)+\left(\frac{474}{497}\right)\left(\frac{1}{\rho}-1\right)\left(\frac{\tau^3}{6}\right)+\left(\frac{\tau^6}{135}\right)+\left(\frac{\tau^{15}}{600}\right)\right]}{D}$ when $\tau=\frac{T}{T_{nell}}<1$
	$1-\frac{\left[\left(\frac{\tau^{-5}}{10}\right)+\left(\frac{\tau^{-15}}{315}\right)+\left(\frac{\tau^{-25}}{600}\right)\right]}{D}$ when $\tau=\frac{T}{T_{nell}}>1$, with ρ=0.28, D=0.34

Previous research shows that the equilibrium constant of NbN and NbC in molten steel at 1500 °C is 0.14 and 14.30, respectively. Nb-containing compounds do not precipitate in molten steel due to their high solubility, but precipitate and grow up in the solid phase after solidification. During the heat treatment at 850~1200 °C, the solid solubility of Nb in austenite can usually be expressed[17] as follows:

$$\lg\left(C_C\cdot C_{Nb}^{0.875}\right) = 2.97 - 7500/T \pm 0.06 \quad (8)$$

where C_C and C_{Nb} are the solid solution contents of C and Nb in austenite, respectively; T is the thermodynamic temperature. In this experiment, the C content of B steel is 1.15wt%, and the solution temperature is 950 °C (1223 K). By Eq.(8), the content of solid-soluted Nb in austenite is only 0.000 27wt%, indicating that almost all of the added

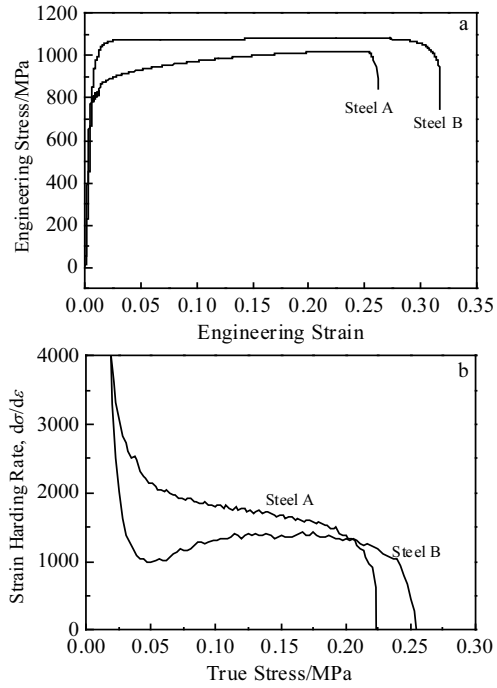

Fig.4 Engineering stress-strain curves (a) and strain hardening rate (dσ/dε)-true stress (b) curves of steel A and steel B steels

Table 3 Mechanical properties of a Fe-28Mn-10Al-C and Fe-28Mn-10Al-C-0.5Nb steels

Steel	YS/MPa	UTS/MPa	EI/%	PSE/GPa·%
A	792	1020	26.0	26.52
B	963	1084	37.5	40.65

Nb in the low-density steel exists as precipitation. Because the steelmaking process is carried out in vacuum, the N content in B steel is extremely low. Moreover, Nb and C have high affinity in steel. Therefore, the added Nb in B steel mainly exists in the form of NbC, which is consistent with the results of SEM and TEM.

3.2 Effect of Nb on grain size

In the process of high temperature treatment, the element diffusion ability improves and the grain boundary migration of the steel increases. Therefore, the austenite grains in low-density steel grow up during the high temperature treatment. As the austenite grain grows, the second phase in the steel cuts off the grain boundary, and produces a drag force for the grain boundary movement. The austenite grain growth is suppressed by the pinning effect of the second phase. In this research, due to the addition of Nb in B steel, NbC phase is precipitated at the austenite grain boundaries and grains. The movement of the grain boundary is hindered due to the pinning effect. As a result, the austenite grains in B steel are obviously refined, and their size is smaller than that of A steel. According to the growth accident theory, the formation probability of twins increases as the grain boundary migrates. The NbC in B steel acts as obstacles to the migration of grain boundary, and suppresses the formation of twins[18,19]. In contrast, A steel shows a relatively high density of twins.

Based on the effect of the second phase of restraining the grain coarsening, the ability of precipitated phases to inhibit grain coarsening is related to their volume fraction and size, and finally determines the degree of austenite grain refinement. The correlation between the volume fraction and size of the second phase with the austenite grain size can be expressed as follows:

$$\gamma_c = 6R_0 f \Big/ \left[\pi(3/2) - 2/Z\right] \quad (9)$$

Where r_c is the critical size of the second phase precipitated in steel, R_0 is the average grain size of austenite grains, f is the volume fraction of the second phase in the steel, and Z is the ratio of the size of grown grain to that of its neighboring grains (usually set as 2). In the process of grain refinement by precipitation of the second phase, the second phase with large volume fraction and small critical size has better grain refinement effect of austenite.

According to the TEM analysis, at the solution temperature of 950 °C, the particle size of NbC is 450 nm in B steel with added Nb. According to the calculated results of Eq.(8), the volume fraction of NbC in B steel is about 0.5wt%. By Eq.(9), through the refinement of NbC, the austenite grain size in Nb-added low-density steel is about 15 μm. This calculation result is basically the same as the result obtained by OM (13.96 μm).

3.3 Correlation between microstructure and tensile properties

In the present study, due to the addition of Nb, the B steel exhibits the improved mechanical properties, such as YS, UTS and EI, in comparison with the A steel. This is determined by the microstructure and precipitate distribution of the two kinds of low-density steels.

Under the external stress, SFE plays a vital role in improving the mechanical properties of Fe-Mn-Al-C low-density steel through changes in deformation mechanism[20,21]. According to the previous research, TRIP effect is the main deformation mechanism of low-density steel when SFE is less than 18 mJ/m^2. With the increase of SFE, deformation twins appear during the deformation process and TWIP effect dominates instead of the martensite transformation. Due to the suppression of twins by high SFE, when SFE exceeds 60 mJ/m^2, the deformation mechanism is dominated by planar slip for the austenitic steel. Based on the previous results, the SFE of A and B steel are 82 and 84 mJ/m^2, respectively, implying that the planar slip is the main deformation mechanism of the two present experimental steels.

In austenitic low-density steel, due to the irregular arrangement of atoms, impurities and defects form at the grain boundaries, resulting in higher energy. Therefore, it will hinders the slippage of dislocations during the deformation process, restrains the plastic deformation, and causes the strengthening of the low-density steel. This behavior is defined as the fine grain strengthening effect. Meanwhile，when the grain size is fine, the number of grain boundaries in the same area increases. Therefore, the deformation occurs in more grains, and the dislocation pile-up and the stress concentration within a single grain reduce, which makes the steel get better fracture toughness. In the present study, because of the grain refinement of NbC, there are more grains in the same area, and the grain boundary density increases. During the deformation, the dislocation slip in B steel is more strongly hindered by the grain boundary compared with A steel, and the dislocation pile-up in a single grain decreases. Thus, in the present study, B steel exhibits the improved mechanical properties than A steel, such as YS, UTS and EI.

In addition to the grain size, the role of NbC precipitation in low-density steel should also be considered. As shown in Fig.2 and 3, due to the addition of Nb in B steel, NbC with the same structure as austenite is precipitated. In the process of tensile deformation, NbC with high hardness plays a role as an obstacle to the dislocation slip, causing precipitation strengthening, so the low-density steel exhibits higher YS and UTS. Meanwhile, the shearing of NbC by dislocations is under consideration. When the dislocation shears the precipitated phase, the structure is destroyed and difficult to recover. Once the leading dislocation shears the precipitate phase, such as NbC, it facilitates the subsequent dislocation to propagate on the same glide plane, which makes it more easily pass through the precipitated phase region on the same plane, promoting the planar slip of dislocation and the form of planar slip bands, and avoiding the stress concentration caused by dislocation pile-up. The softening phenomenon is also referred as glide plane softening[22,23]. It is worth noting that the interaction between NbC and dislocation slip does not alter the planar slip mode in low-density steel. Thus, the interaction between NbC and dislocation slip in B steel can delay the plastic instability. The B steel has higher EI in comparison to steel A without Nb.

In addition, the grain size of A steel is larger and no precipitates form due to the absence of Nb. The stress required for dislocation slip is small. In the initial stage of plastic deformation, the density of dislocations in A steel increases rapidly under the same stress conditions. Plenty of dislocations pile up at grain boundaries and defects, causing stress concentration, so the strain hardening rate of A steel is higher than that of B steel. With the increase of the strain, B steel maintains continuous high $d\sigma/d\varepsilon$ values due to the fine grain strengthening and glide plane softening. Thus, the plastic instability is delayed, causing that the B steel obtains better strain hardening ability.

Based on the previous analyses, the refinement of austenite grain and the precipitation of NbC in B steel can simultaneously improve the plasticity and toughness of austenitic low-density steel. In particular, the addition of Nb improves the YS (increment of 171 MPa) of low-density steel. To investigate the effects of precipitation strengthening and fine grain strengthening, based on the Gladman's theory[24] and Ashby-Orowan's modified model, the contribution of precipitation strengthening on YS of B steel can be calculated as follows:

$$\Delta\sigma_{\mathrm{P}}=\frac{0.538Gbf^{1/2}}{D}\ln\left(\frac{D}{2b}\right) \tag{10}$$

where, $\Delta\sigma_{\mathrm{p}}$ is the YS increment caused by precipitation strengthening of the second phase (NbC) in low-density steel; G is the shear modulus, the value of which in iron matrix usually set as 81 600 MPa; b is the Burgers vector mode, the value of which in iron matrix is 0.248 nm; f is the volume fraction of the precipitated second phase (NbC), which is 0.5% calculated by Eq.(8); D is the diameter of the precipitated phase NbC (450 nm). Taking the values into Eq.(10), the YS increment of B steel caused by NbC precipitation strengthening is 116.5 MPa, indicating that the increase of YS of Nb-added low-density steel is mainly caused by the precipitation strengthening.

4 Conclusions

1) Nb exists as NbC in austenitic Fe-Mn-Al-C low-density steel. The NbC in the low-density steel has the same structure as the austenite, and is distributed in the austenite grains and at the grain boundaries with an ellipsoidal shape and the grain size of about 450 nm.

2) As the 0.5wt% Nb is added into Fe-28Mn-10Al-C low-density steel, the average austenite grain size is refined from 39.49 μm to 13.67 μm, and the number of twins also reduces.

3) When 0.5wt% Nb is added into Fe-28Mn-10Al-C low-density steel, the YS and UTS increase by 171 and 64 MPa, respectively, EI increases by 11.5%, and the strength and ductility show a good balance, i.e., the product of strength and elongation reaches 40.65 GPa·%.

4) Both the Fe-28Mn-10Al-C and Fe-28Mn-10Al-C-0.5Nb low-density steels have high stacking fault energy, and the dominant deformation mechanism of the Nb-added low-density steels is planar slip. The high strength and toughness of Nb-containing low-density steel are related to the precipitation strengthening effect of the NbC and the fine grain strengthening. The increase of YS of Nb-added low-density steel is mainly caused by precipitation strengthening.

References

1 Moon J, Park S J, Jang J H *et al*. *Scripta Materialia*[J], 2017, 127: 97

2 Xing J, Wei Y H, Hou L F. *Journal of Metals*[J], 2018, 70(6): 929

3 Song H, Yoo J, Kim S H *et al*. *Acta Materialia*[J], 2017, 135: 215

4 Yang M X, Yuan F P, Xie Q G *et al. Acta Materialia*[J], 2016, 109: 213

5 Li X, Ma T, Cao Y P *et al*. *Hot Working Technology*[J], 2018, 47(6): 15 (in Chinese)

6 Allain S, Chateau J P, Bouaziz O. *Materials Science and Engineering A*[J], 2004, 387-389: 143

7 Sutou Y, Kamiya N, Umino R *et al. ISIJ International*[J], 2010, 50(6): 893

8 Kalashnikov I S, Acselrad O, Pereira L C. *Journal of Materials Engineering and Performance*[J], 2000, 9: 597

9 Moon J, Ha H Y , Park S J *et al*. *Journal of Alloys and Compounds*[J], 2019, 775: 1136

10 Jeong S, Park G, Kim B *et al*. *Materials Science and Engineering A*[J], 2019, 742: 61

11 Lu W J, Zhang X F, Qin R S. *Materials Letters*[J], 2015, 138: 96

12 Liu D G, Cai M H, Ding H *et al*. *Materials Science and Engineering A*[J], 2018, 715: 25

13 Li H Z, Zhang X W, Zhu C L *et al*. *Rare Metal Materials and Engineering*[J], 2016, 45(7): 1740 (in Chinese)

14 Tian H, Zhou J, Gong W J *et al*. *Rare Metal Materials and Engineering*[J],2017, 46(12): 3994 (in Chinese)

15 Yoo J D, Park K T. *Materials Science and Engineering A*[J], 2008, 496: 417

16 Narita K, Koyama S. *Kobe Steel Engineering Report*[J], 1966, 16: 179

17 Yong Q L, Zheng L, Sun Z B. *Acta Metallurgica Sinica*[J], 1986, 22(6): 81

18 Mahajan S, Pande C S, Imam M A *et al*. *Acta Materialia*[J], 1997, 45: 2633

19 Pande C S, Imam M A, Rath B B *et al*. *Metallurgical and Materials Transactions A*[J], 1990, 21: 2891

20 Zhu Y T, Wu X L, Liao X Z *et al*. *Acta Materialia*[J], 2011, 59(2): 812

21 Saeed-Akbari A, Imlau J, Prahl U *et al*. *Metallurgical and Materials Transaction A*[J], 2009, 40: 3076

22 Parka k, Jin K G, Han S H *et al*. *Materials Science and Engineering A*[J], 2010, 527: 3651

23 Welsch E, Ponge D, Haghighat S M H *et al. Acta Materialia*[J], 2016, 116: 188

24 Gladman T. *Materials Science and Technology*[J], 1999, 15 (1): 30

Nb 对 Fe-28Mn-10Al-C 低密度钢组织与机械性能的影响

马 涛[1]，高建新[1]，李慧蓉[1]，孟祥海[1,2]，李运刚[1]

(1. 华北理工大学 冶金与能源学院，河北 唐山 063210)

(2. 唐山工业职业技术学院，河北 唐山 063210）

摘　要：开发制备了一种汽车用含 0.5%Nb（质量分数）的 Fe-28Mn-10Al-C-0.5Nb 低密度钢，旨在研究 Nb 在奥氏体 Fe-Mn-Al-C 低密度钢中的存在形态，以及 Nb 添加对 Fe-Mn-Al-C 低密度钢组织与力学性能影响。结果表明，Fe-28Mn-10Al-C 低密度钢中加入 Nb 后，奥氏体晶粒平均尺寸由 39.49 μm 细化到 13.67 μm，且退火孪晶形成受到抑制。随着 Nb 添加，Fe-28Mn-10Al-C 低密度钢的屈服强度和抗拉强度分别升高 170 MPa 和 64 MPa，断后伸长率升高 11.5%，强度与延展性表现出良好平衡。加 Nb 低密度钢的高强度与高韧性与 NbC 析出相的沉淀强化和奥氏体细晶强化有关，且含 Nb 低密度钢屈服强度的升高主要由析出强化引起。

关键词：Fe-Mn-Al-C；Nb；NbC；晶粒细化；拉伸性能

作者简介：马 涛，男，1990 年生，博士生，华北理工大学冶金与能源学院，河北 唐山 063210，E-mail: matao2011@sina.com